Inverse scattering for near-field microscopy

P. Scott Carney[a] and John C. Schotland
Department of Electrical Engineering, Washington University, St. Louis, Missouri 63130

(Received 8 June 2000; accepted for publication 31 August 2000)

We derive the analytic singular value decomposition of the linearized scattering operator for scalar waves. This representation leads to a robust inversion formula for the inverse scattering problem in the near zone. Applications to near-field optics are described. © *2000 American Institute of Physics.* [S0003-6951(00)00244-8]

There has been considerable recent interest in the development of near-field methods for optical microscopy.[1,2] This interest is motivated by the remarkable ability of such methods to image spatial structure with subwavelength resolution.[3–8] It is now well recognized, however, that the analysis and interpretation of near-field images is somewhat problematic. The difficulty can be traced to the fact that the connection between the image and the three-dimensional structure of the sample has not been made clear. In particular the effects of variations in topography and the optical properties of the sample have proven to be indistinguishable.[9] For this reason there is substantial interest in the near-field inverse scattering problem. To date, work in this direction has been limited to the study of surface profile reconstruction for homogeneous media.[9–12]

In this letter we present an analytic solution to the linearized near-field inverse scattering problem for three-dimensional inhomogeneous media. This result is particularly timely in view of the recent publication in this journal of a landmark letter[13] demonstrating the experimental realization of measurements of the optical phase in the near zone. Such measurements provide the necessary input data for the near-field inverse scattering problem. Our solution to this problem has the form of an explicit inversion formula and is obtained from the observation that it is possible to construct the singular value decomposition (SVD) of the scattering operator. This approach provides considerable insight into the mathematical structure of the inverse problem and provides a natural means of regularization which sets the resolution of the reconstructed image to be commensurate with the available data.

We begin by considering an experiment in which a monochromatic plane wave is incident on a medium described by a scattering potential $V(\mathbf{r})$. For simplicity, we ignore the effects of polarization and consider the case of a scalar wave. The field $U(\mathbf{r})$ satisfies the reduced wave equation, $\nabla^2 U + k_0^2 U = -VU$ where $k_0 = 2\pi/\lambda$ is the free-space wave number. Following standard procedures, we find that the scattered wave $U_s(\mathbf{r})$ produced on scattering of an incident unit amplitude propagating plane wave with wave vector $\mathbf{k}$ may be expressed to lowest order in perturbation theory in V as

$$U_s(\mathbf{r}) = \int d^3r' \, e^{i\mathbf{k}\cdot\mathbf{r}'} G(\mathbf{r}-\mathbf{r}') V(\mathbf{r}'), \tag{1}$$

where $G(\mathbf{r}) = e^{ik_0 r}/4\pi r$ is the outgoing Green's function.

We assume that the scattered wave is measured on the plane $z = z_d$ with the scatterer taken to lie entirely in the region $0 \leqslant z \leqslant z_{\max}$. We consider either the transmission geometry where $z_d \geqslant z_{\max}$, or the reflection geometry where $z_d = 0$. We denote the transverse part of the wave vector of the incident field by $\mathbf{q}$ so that $\mathbf{k} = [\mathbf{q}, k_z(\mathbf{q})]$, $k_z(\mathbf{q}) = \sqrt{k_0^2 - q^2}$. We also denote the transverse spatial coordinate by $\boldsymbol{\rho}$, and the scattered field in the plane $z = z_d$ by $U_{\mathbf{q}}(\boldsymbol{\rho})$. It will prove useful to express the Green's function in a plane wave decomposition:

$$G(\mathbf{r}) = \frac{i}{2(2\pi)^2} \int d^2Q \, k_z(\mathbf{Q})^{-1} \exp\{i\mathbf{Q}\cdot\boldsymbol{\rho} + ik_z(\mathbf{Q})|z|\}, \tag{2}$$

where $\mathbf{r} = (\boldsymbol{\rho}, z)$. The waves corresponding to $Q^2 \leqslant k_0^2$ are the homogeneous plane waves and the waves corresponding to $Q^2 > k_0^2$ are the evanescent waves. In the far field, the effect of evanescent waves can be neglected and only the low-frequency part of the Green's function contributes to $U_{\mathbf{q}}(\boldsymbol{\rho})$. As a consequence, we recover the well known diffraction-limited resolution of $\lambda/2$.[14] In the near field, both low and high frequency parts of the scattered wave contribute to $U_{\mathbf{q}}(\boldsymbol{\rho})$ which leads to improved spatial resolution.

In the inverse scattering problem we wish to reconstruct $V(\mathbf{r})$ from measurements of $U_{\mathbf{q}}(\boldsymbol{\rho})$. We consider a discrete set of incident plane waves labeled by their transverse wave vectors $\mathbf{q}$. The image reconstruction problem consists of solving the system of integral equations

$$U_{\mathbf{q}}(\boldsymbol{\rho}) = \int d^3r' \, A_{\mathbf{q}}(\boldsymbol{\rho}, \mathbf{r}') V(\mathbf{r}'), \tag{3}$$

where $A_{\mathbf{q}}(\boldsymbol{\rho}, \mathbf{r}')$ is defined by Eqs. (1) and (2) for each wave vector. The solution to Eq. (3) follows from the SVD of the vector valued operator A whose components are the integral operators $A_{\mathbf{q}}$, the SVD being given by

$$\mathbf{A}(\boldsymbol{\rho}, \mathbf{r}') = \int d^2Q \sum_{\ell} \sigma_{\mathbf{Q}\ell} \phi_{\mathbf{Q}\ell}(\boldsymbol{\rho}) \psi^*_{\mathbf{Q}\ell}(\mathbf{r}'). \tag{4}$$

Here the singular functions $\phi_{\mathbf{Q}\ell}(\boldsymbol{\rho}_1)$ and $\psi_{\mathbf{Q}\ell}(\mathbf{r})$, and singular values $\sigma_{\mathbf{Q}\ell}$ are defined by

$$\mathbf{A}^*\mathbf{A}\psi_{\mathbf{Q}\ell} = \sigma^2_{\mathbf{Q}\ell}\psi_{\mathbf{Q}\ell}, \tag{5}$$

$$\mathbf{A}\psi_{\mathbf{Q}\ell} = \sigma_{\mathbf{Q}\ell}\boldsymbol{\phi}_{\mathbf{Q}\ell}. \tag{6}$$

[a]Electronic mail: scott@ee.wustl.edu

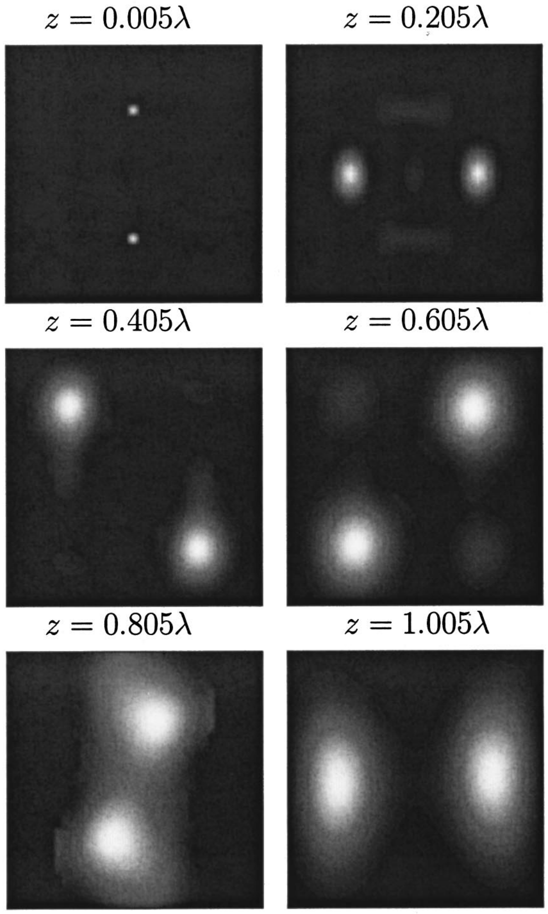

FIG. 1. Tomographs at distances z from the measurement plane. The field of view in each tomograph is $\lambda \times \lambda$.

In order to solve Eqs. (4)–(6) for ψ and ϕ it will prove useful to first find the SVD of $A_{\mathbf{q}}(\rho,r')$. We find that

$$A_{\mathbf{q}}(\boldsymbol{\rho},\mathbf{r}') = \int d^2Q\, \sigma_{\mathbf{Q}}^{\mathbf{q}} g_{\mathbf{Q}}^{\mathbf{q}}(\boldsymbol{\rho}) f_{\mathbf{Q}}^{\mathbf{q}*}(\mathbf{r}'), \tag{7}$$

where

$$g_{\mathbf{Q}}^{\mathbf{q}}(\boldsymbol{\rho}) = \frac{1}{2\pi} e^{i(\mathbf{Q}+\mathbf{q})\cdot\boldsymbol{\rho}}, \tag{8}$$

$$f_{\mathbf{Q}}^{\mathbf{q}}(\mathbf{r}) = \frac{-iB(z)}{4\pi\sigma_{\mathbf{Q}}^{\mathbf{q}} k_z^*(\mathbf{Q}+\mathbf{q})} \times \exp\{i\mathbf{Q}\cdot\boldsymbol{\rho} - i|z-z_d| k_z^*(\mathbf{Q}+\mathbf{q}) - izk_z^*(\mathbf{q})\}, \tag{9}$$

where $B(z)$ is a function which is unity on the interval $z \in [0,z_{\max}]$ and is zero elsewhere. This result can be used to obtain the identity $A_{\mathbf{q}}^* A_{\mathbf{q}} f_{\mathbf{Q}}^{\mathbf{q}'} = \chi_{\mathbf{qq}'}(\mathbf{Q})(\sigma_{\mathbf{Q}}^{\mathbf{q}})^2 f_{\mathbf{Q}}^{\mathbf{q}}$, where the overlap function $\chi_{\mathbf{qq}'}(\mathbf{Q})$ is defined by the expression $\langle f_{\mathbf{Q}}^{\mathbf{q}}, f_{\mathbf{Q}'}^{\mathbf{q}'}\rangle = \chi_{\mathbf{qq}'}(\mathbf{Q})\,\delta^{(2)}(\mathbf{Q}'-\mathbf{Q})$. An explicit expression for $\sigma_{\mathbf{Q}}^{\mathbf{q}}$ may be found but is not needed.

Returning now to the problem of constructing the SVD of $\mathbf{A}$, we make use of Eq. (5) and the ansatz that $\psi_{\mathbf{Q}\ell}(\mathbf{r}) = \sigma_{\mathbf{Q}\ell}^{-1} \Sigma_{\mathbf{q}} \sigma_{\mathbf{Q}}^{\mathbf{q}} c_{\ell\mathbf{q}}(\mathbf{Q}) f_{\mathbf{Q}}^{\mathbf{q}}(\mathbf{r})$, to find that the vectors of coefficients $\mathbf{c}_{\ell}(\mathbf{Q})$ are the eigenvectors with eigenvalues $\sigma_{\mathbf{Q}\ell}^2$ of a matrix $M(\mathbf{Q})$ given by the expression $M_{\mathbf{qq}'}(\mathbf{Q}) = \chi_{\mathbf{qq}'}(\mathbf{Q})\sigma_{\mathbf{Q}}^{\mathbf{q}}\sigma_{\mathbf{Q}}^{\mathbf{q}'}$, explicitly

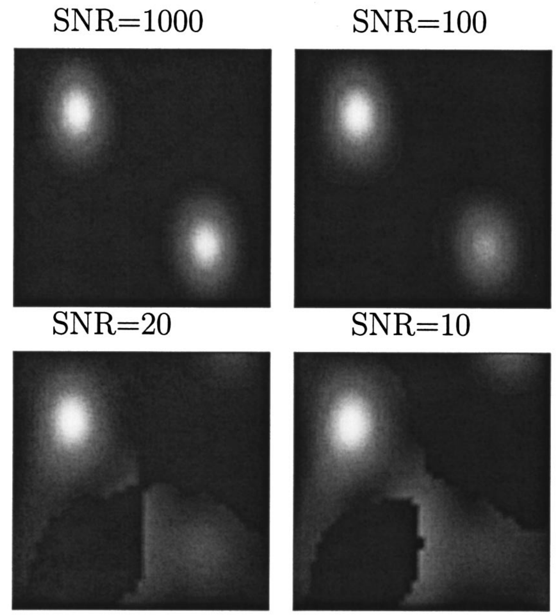

FIG. 2. Tomographs of a scatterer consisting of two point scatterers a distance 0.51λ from the detector with signal to noise ratios (SNR) as indicated. The SNR is the ratio of magnitude of the signal to the standard deviation of the noise at each data point.

$$M_{\mathbf{qq}'}(\mathbf{Q}) = \frac{i e^{i\varepsilon z_d[k_z(\mathbf{q}'+\mathbf{Q}) - k_z^*(\mathbf{q}+\mathbf{Q})]}}{4k_z(\mathbf{q}'+\mathbf{Q})k_z^*(\mathbf{q}+\mathbf{Q})} \times \frac{1 - e^{iz_{\max}[\varepsilon k_z^*(\mathbf{q}+\mathbf{Q}) + k_z^*(\mathbf{q}) - \varepsilon k_z(\mathbf{q}'+\mathbf{Q}) - k_z(\mathbf{q}')]}}{\varepsilon k_z^*(\mathbf{q}+\mathbf{Q}) + k_z^*(\mathbf{q}) - \varepsilon k_z(\mathbf{q}'+\mathbf{Q}) - k_z(\mathbf{q}')}, \tag{10}$$

where $\varepsilon = 1$ for the transmission geometry and $\varepsilon = -1$ for the reflection geometry ($z_d = 0$). Since $M(\mathbf{Q})$ is Hermitian we can choose the $\mathbf{c}_{\ell}(\mathbf{Q})$ to be orthonormal. It may now be obtained from Eq. (6) that the $\phi_{\mathbf{Q}\ell}(\mathbf{r})$ are given by $\phi_{\mathbf{Q}\ell\mathbf{q}'}(\boldsymbol{\rho}) = c_{\ell\mathbf{q}'}(\mathbf{Q}) g_{\mathbf{Q}}^{\mathbf{q}'}(\boldsymbol{\rho})$. The solution to Eq. (3) may now be expressed as

$$V(\mathbf{r}) = \int d^2\rho' \mathbf{A}^+(\mathbf{r},\boldsymbol{\rho}')\mathbf{U}(\boldsymbol{\rho}'), \tag{11}$$

where

$$\mathbf{A}^+(\mathbf{r},\boldsymbol{\rho}') = \int d^2Q \sum_{\ell} \frac{1}{\sigma_{\mathbf{Q}\ell}} \psi_{\mathbf{Q}\ell}(\mathbf{r}) \phi_{\mathbf{Q}\ell}^*(\boldsymbol{\rho}'), \tag{12}$$

is the generalized inverse of $\mathbf{A}(\boldsymbol{\rho},\mathbf{r}')$. Finally, using Eqs. (11) and (12) we obtain our main result:

$$V(\mathbf{r}) = \int d^2\boldsymbol{\rho}' \int d^2Q \sum_{\ell,\mathbf{q}} \frac{1}{\sigma_{\mathbf{Q}\ell}} \psi_{\mathbf{Q}\ell}(\mathbf{r}) \phi_{\mathbf{Q}\ell\mathbf{q}}^*(\boldsymbol{\rho}') U_{\mathbf{q}}(\boldsymbol{\rho}'), \tag{13}$$

or explicitly,

$$V(\mathbf{r}) = \frac{-i}{2(2\pi)^2} \int d^2Q \sum_{\mathbf{q},\mathbf{q}',\ell} \frac{1}{\sigma_{\mathbf{Q}\ell}^2} c_{\ell\mathbf{q}'}^{\mathbf{Q}} c_{\ell\mathbf{q}}^{\mathbf{Q}*} \times \exp\{i\mathbf{Q}\cdot\boldsymbol{\rho} - i|z-z_d| k_z^*(\mathbf{q}'+\mathbf{Q}) - izk_z^*(\mathbf{q}')\} \times \tilde{U}_{\mathbf{q}}(\mathbf{q}+\mathbf{Q}), \tag{14}$$

where $\tilde{U}_{\mathbf{q}}(\mathbf{Q})$ is the two dimensional Fourier transform of $U_{\mathbf{q}}(\boldsymbol{\rho})$.

The above formula gives the minimum L^2 norm solution to the inverse problem given the scattering data. This statement follows from the result that the SVD provides the solution to Eq. (3) that belongs to the orthogonal complement of the null space. It is important to note that the size of the null space is expected to decrease as the number of incident wave vectors increases and thus the inversion procedure is systematically improvable. Additionally the SVD provides considerable information on the degree of ill posedness of the problem through the rate of decay of the singular values. It also gives insight into how much information is contained in the data by controlling which features of V can be recovered in a stable way, namely those that are close to a singular function with correspondingly large singular value.

The inversion kernel Eq. (12) is highly singular, and thus numerically unstable. As a consequence, it is necessary to introduce a cutoff on the small singular values thereby effecting a regularization of the inverse problem. That is, we set $\psi_{\mathbf{Q}\ell}=\phi_{\mathbf{Q}\ell}=0$ for $\sigma_{\mathbf{Q}\ell}<\sigma_{\min}$, where $\sigma_{\min}$ must be chosen appropriately for the available data. Note that regularization here has a natural physical interpretation—it simply sets the spatial resolution of the reconstruction.

To demonstrate the feasibility of the reconstruction algorithm, we have numerically simulated the forward problem to obtain the data for measurements made in a transmission geometry. The scatterer consists of a three-dimensional distribution of twelve point scatterers, two on the horizontal, vertical, or diagonal axis of each of six planes. Figure 1 shows the reconstructions obtained. Because the high frequency components of the field fall off exponentially with distance from the scatterer, the resolution of the image is dependent on the depth of the slice. The simulations were done for 21 angles of illumination with transverse wave vectors all directed in the $\hat{\mathbf{x}}$ direction and ranging uniformly from $-k_o\hat{\mathbf{x}}$ to $k_0\hat{\mathbf{x}}$. The inversion kernel [Eq. (12)] was obtained by computing the matrices M from expression (10) and numerically diagonalizing to obtain the $\mathbf{c}_\ell^{\mathbf{Q}}$ and $\sigma_{\mathbf{Q}\ell}$. It is important to note that this is a one time computational cost. The sum on ℓ was truncated for $\sigma^2_{\mathbf{Q}\ell}<\max(\sigma^2_{\mathbf{Q}\ell})\times 10^{-7}$. The Fourier transform of the field $\tilde{U}_{\mathbf{q}}(\mathbf{Q})$ was computed for vectors $\mathbf{Q}$ on a 41 by 41 grid with a spacing of $0.5k_0$. The images are displayed on a quadratic gray scale and negative values of the reconstructed potential have been rejected.

Figure 2 demonstrates the robustness of the inversion procedure in the presence of noise. We present the reconstruction of two point scatterers a distance 0.51λ from the measurement plane with noise added to the signal at various levels as indicated. The noise was taken to be Gaussian and of zero mean, with a variance proportional to the square of the signal at each pixel on the measurement plane.

In conclusion, we have described an inverse scattering method for near-field scattered waves that provides subwavelength resolution. We emphasize that our approach represents an analytic rather than a numerical solution to the image reconstruction problem. The recent demonstration of phase measurements in the optical near field[13] suggests that the idea presented here is experimentally feasible. Furthermore, our results are of general physical interest since they are applicable to imaging with any scalar wave with data obtained in any zone.

The authors wish to thank Dr. Vadim Markel for valuable discussions.

[1] C. Girard and A. Dereux, Rep. Prog. Phys. **59**, 657 (1996).
[2] D. Courjon and C. Bainier, Rep. Prog. Phys. **57**, 989 (1994).
[3] E. Synge, Philos. Mag. **6**, 356 (1928).
[4] E. Ash and G. Nicholls, Nature (London) **237**, 510 (1972).
[5] A. Lewis, M. Isaacson, A. Harootunian, and A. Muray, Ultramicroscopy **13**, 227 (1984).
[6] D. W. Pohl, W. Denk, and M. Lanz, Appl. Phys. Lett. **44**, 651 (1984).
[7] E. Betzig and J. K. Trautman, Science **257**, 189 (1992).
[8] R. Dickson, D. Norris, Y. L. Tzeng, and W. Moerner, Science **274**, 966 (1996).
[9] J.-J. Greffet, A. Sentenac, and R. Carminati, Opt. Commun. **116**, 20 (1995).
[10] N. Garcia and M. Nieto-Vesperinas, Opt. Lett. **18**, 2090 (1993).
[11] N. Garcia and M. Nieto-Vesperinas, Opt. Lett. **20**, 949 (1995).
[12] R. Carminati, J.-J. Greffet, N. Garcia, and M. Nieto-Vesperinas, Opt. Lett. **21**, 501 (1996).
[13] P. L. Phillips, J. C. Knight, J. M. Pottage, G. Kakarantzas, and P. St. J. Russel, Appl. Phys. Lett. **76**, 541 (2000).
[14] E. Wolf, Opt. Commun. **1**, 153 (1969).